COMPARISON OF THREE MEASURES OF VISIBILITY EXTINCTION IN DENVER, COLORADO

John G. Watson
Judith C. Chow
Lyle C. Pritchett

Desert Research Institute
University of Nevada System
Reno, NV 89506

L. Willard Richards
Sonoma Technology, Inc.
Santa Rosa, CA

David L. Dietrich
John Molenar
John Faust
Air Resources Specialists
Ft. Collins, CO

Stephen R. Andersen
ENSR Consulting and Engineering
Ft. Collins, CO

Christine Sloane
General Motors Research Laboratory
Dearborne, MI

INTRODUCTION

Sight-path measurements of light extinction are needed to relate the extinction along that path to human perception. This is the case because visibility impairment is perceived only when objects are viewed at great distances, not when they are right next to the observer. Measurement technology to quantify visibility-reducing atmospheric constituents along a sight path does not yet exist, however. These constituents must be measured at a fixed sampling point. Measurements of extinction are also needed at a collocated point to establish a relationship between extinction and atmospheric constituents and between the point and sight-path measurements of light extinction.

When the extinction efficiencies (extinction per unit concentration) for different chemical constituents are known, light extinction can be calculated from those concentrations. These same atmospheric constituents can often be used in receptor models to estimate source contributions. When all of these measures are combined, the source contribution of each pollution source type to sight-path light extinction can be estimated. The goal of this presentation is to compare atmospheric light extinction obtained from: 1) transmissometer measurements along a sight path (termed PATH extinction); 2) nephelometer, particle absorption, and nitrogen dioxide absorption measurements at a point (termed POINT extinction); and 3) fine particle chemical measurements apportioned to source contributors at a point (termed POINT extinction) .

MEASUREMENTS

Five measurement systems were collocated atop the 75 m (AGL) Federal Building in downtown Denver, CO, during the 1987-88 Metro Denver Brown Cloud Study: 1) a sight-path transmissometer; 2) an integrating nephelometer; 3) a chemiluminescent nitrogen oxides analyzer; 4) a fine particle sequential filter sampler; and 5) a Micro-Orifice Uniform Deposit Impactor. These systems acquired the measurements needed to determine visibility extinction along a sight-path (PATH), at a point at one end of the sight path (POINT), and from point measurements of atmospheric constituents (CHEMICAL).

Measurements were taken continuously from November 2, 1987 through February 1, 1988. The operation of these instruments and the precision, accuracy and validity of their measurements are described in detail by Watson et al.[1,2,3]. The following summaries emphasize method and operational differences and limitations which could result in differences in extinction among the different methods.

Transmissometer

An Optec LRT-2 long-range transmissometer was used to measure sight-path extinction. This transmissometer consists of a constant output modulated light source transmitter and a computer-controlled photometer receiver with a 530 nm narrow bandpass filter. The receiver was located atop the 75 m above ground level (AGL) Federal Building and the transmitter was positioned atop an apartment building of similar height at a distance of 2.7 km SE of the receiver.

One-minute averages were accumulated and recorded as 10-minute averages. This signal averaging reduces the variability caused by random changes in transmittance caused by atmospheric turbulence. Hourly average extinction values were generated from these ten minute averages. The LRT-2 was calibrated by measuring the intensity of the same light source at two distances. A mask was placed over the receiver for the shorter distance so that the observed solid angle equalled that viewed for the longer distance.

The exterior optical surfaces were cleaned and the alignment of both the transmitter and receiver were checked weekly. Hourly averages were adjusted for changes in the source intensity due to lamp aging. An automated photographic system documented weather and sun conditions with hourly 35 mm slides. Extinction values were invalidated when: 1) snow, fog, or rain obscured the light from the transmitter; 2) condensation on the receiver lens was excessive; and 3) when the instrument malfunctioned.

Nephelometers

The MRI Model 1560 Integrating Nephelometer was used to monitor particle scattering coefficient atop the Federal Building. The integrating nephelometer provides a point measure of the light scattered by particles and gases in a sample volume integrated over a hemisphere for a weighted range of visible wavelengths. The MRI 1560 nephelometer measures light scattering at wavelengths of 525 to 530 nm with a ~50 nm bandwidth. The MRI 1560 was calibrated with clean air, Freon-11 and Freon-22. Performance tests with one of these gases were conducted weekly. A gently curving three-inch diameter PVC pipe served as the sample inlet. The approximate cutpoint of inlets of this type is generally in the neighborhood of 15 to 20 μm.

The MRI 1560 is intended to be operated in environmentally controlled shelters. This operation causes the temperature of the sample volume to be near the temperature of the shelter rather than the temperature of the air being sampled. Air in the sample volume is further heated by the nephelometer lamp. This heating lowers the relative humidity (RH) in the sample volume with respect to the RH of the air in which the particles are suspended. This difference in RH changes the liquid water content and the light scattering properties of soluble particles. These changes are significant when relative humidities exceed 70% and the difference between nephelometer and ambient temperatures exceeds 2 °C. The MRI 1560 used in this project was operated at shelter temperatures from 11/2/87 to 11/20/87 with continuous temperature probes in ambient air, at the sample inlet to the shelter, and in the sample chamber. The sample chamber was found to exceed ambient temperatures by more than 10 °C, and this was deemed unacceptable.

To minimize these temperature differences, the nephelometer was relocated on 11/20/87 inside a plywood enclosure which was ventilated with a 16-inch exhaust fan. This fan bathed the entire nephelometer and its built-in electronics with a volume of ambient air which was replaced approximately once every second. This configuration reduced temperature differences inside the

nephelometers to 1 to 2 °C above ambient, thereby minimizing the loss of liquid water in the suspended particles.

The lowest of two ten-minute auto-zero values, taken every six hours, was subtracted from the nephelometer output for the corresponding six-hour period. This baseline adjustment assumes that the zero value drifts linearly from one auto-zero to the next (six hours later). Negative values resulting from this adjustment were set to zero. Hourly average particle scattering values were calculated from the ten-minute averages when three or more valid ten-minute averages were available.

Ruby and Waggoner[4] report that the MRI 1560 responds to a wavelength range between 480 and 600 nm with a peak response near 530 nm. This differs slightly, but not significantly, from the 550 nm wavelength used by the transmissometer. The MRI 1560 measures the amount of light scattered through angles smaller than about 7 degrees or larger than about 165 degrees[5,6] and is blind to light scattered through angles near zero and 180 degrees. Most of the light scattered by the $PM_{2.5}$ size fraction is measured by the MRI 1560, but larger particles scatter preferentially in the forward direction. The scattering by coarse particles (larger than 2.5 μm in aerodynamic diameter) is generally underestimated by a factor of two.

Sequential Filter Samples

The sequential filter sampler (SFS) draws air through a cyclone with a 2.5 μm 50% cutpoint. Nuclepore filter holders with Viton O-rings were located inside the plenum and connected to solenoid valves with quick-disconnect fittings. A timer switched the suction from one set of filters to another to acquire sequential samples from 0900 to 1600 MST over the entire sampling period.

Simultaneous samples were taken on pre-fired quartz and Teflon membrane filter media at 20 l/min. The remaining 73 l/min required for the 113 l/min fine particle inlet was drawn through a makeup air port inside the plenum. The timer was set to cycle sequentially between five sampling ports. The sixth sampling port activated a stepper switch reset which returns sampling to port one. Four filter pack sets were changed every 48 hours while a fifth set was sampling. The 10-minute loss of sampling during changeout did not adversely affect the sample in progress.

Flow rates were set with a calibrated rotameter and were monitored with the same rotameter on each site visit. A differential pressure regulator compensated for changes in flow rate with filter loading. Unexposed filters were loaded into filter holders in the laboratory into filter holders and were unloaded immediately after sampling and placed under refrigeration to minimize changes in the sample prior to analysis.

The Teflon filter was submitted to gravimetric and x-ray fluorescence analyses for total mass and 35 elemental concentrations. Half of the quartz filter was extracted in deionized distilled water and this extract was submitted to anion chromatography for sulfate and nitrate, automated colorimetry for ammonium, and atomic absorption spectrophotometry for potassium. Portions of

the remaining half were submitted to thermal/optical reflectance analysis for organic and elemental carbon. One out of each samples was analyzed as a replicate. Accuracy was determined by an independent audit.

Particle absorption was determined by the attenuation of light transmitted through the Teflon membrane and quartz fiber filters. Each filter was placed in a jig over a specularly diffused vertical light beam in a Tobias Associates densitometer. The spectral distribution of the transmitted light for this system is approximately Gaussian, peaking near 550 nm with full width at half maximum of about 150 nm. The detector is positioned at a constant height above the filter with a shim to prevent contact with the filter itself. The filter optical density was measured on each filter before and after sampling and these two values were converted to absorption. The densitometer was calibrated with neutral density filters, and one of these standards was analyzed every 10 filters to verify instrument stability. Replicate analyses were performed on one out of every ten samples.

Intercomparisons among different filter transmission methods have shown high correlations of absorption, but up to factors of two differences in absolute values. These differences are functions of: 1) the type of filter; 2) filter loading; 3) the chemical and physical nature of the deposit; 4) the wavelengths of light used; 5) calibration standards; and 6) light diffusing methods. At the current time there is no agreement on which combination most accurately represents light absorption in the atmosphere. It has been shown both experimentally[7] and theoretically[8] that when particles are imbedded in a disk (such as a filter), their effective absorption coefficient depends on whether the illumination is collimated or diffuse. Also, the effective absorption coefficient for perfectly diffuse radiation is twice that for completely collimated radiation. The absorption measured on the quartz filters was approximately twice that measured on the Teflon membrane filters, which is consistent with the diffusing properties of the quartz fiber filter. The relationship between the Teflon filter absorption and elemental carbon was approximately 9 m^2/g which is consistent with commonly accepted values. The absorption measured on the Teflon filter was selected for use in this study.

Nitrogen Oxides Monitor

Light-absorbing nitrogen dioxide was measured with a TECO 14B/E nitrogen oxides chemiluminescent monitor. This model is an EPA equivalent method which draws ambient air into a chamber where ozone is introduced to produce electronically excited NO_2 and oxygen. When the excited NO_2 returns to the ground state, it emits radiation with an intensity proportional to the NO concentration. This radiation is monitored with a photomultiplier tube. Alternate measurements of ambient air, and air which has passed through a NO_2 to NO converter, are made. The NO_2 is determined by difference between the NO_x and NO measurements. Nitric acid and PAN have been found to interfere with this measurement[9]). Ambient concentrations of these interferents in wintertime Denver are not expected to be present at levels which would cause significant biases.

The TECO 14B/E was calibrated and operated according to EPA procedures[10]). Standard NO gas concentrations from a certified cylinder were diluted to known concentrations with clean air and presented to the instrument inlet for calibration and performance testing. NO_2 was produced by gas-phase titration in the calibration system. Single point performance tests were performed weekly and the instrument was recalibrated when instrument response exceeds the challenge value by more than 10%.

Micro Orifice Uniform Deposit Impactor

The Micro Orifice Uniform Deposit Impactor (MOUDI) acquires size-resolved particle deposits on substrates amenable to mass, carbon and ion deposits on substrates which are amenable to mass, carbon, sulfate and nitrate analyses. The MOUDI consists of a stack of impactor jets and impaction surfaces which have been especially designed to obtain sharp cutpoints in the particle size range (0 to 3 μm) of greatest importance for visibility impairment. The impaction jets consist of thin metal plates with hundreds of closely space microscopic holes at the lower size ranges. A removable impaction plate is located underneath these jets for placement of a appropriate substrates. The nine size ranges offered by the two MOUDIs used in this study were 1.78 to 3.16 μm, 1.0 to 1.78 μm, 0.56 to 1.0 μm, 0.28 to 0.56 μm, 0.17 to 0.28 μm, 0.072 to 0.17 μm, 0.036 to 0.072 μm, and less than 0.032 μm.

Two MOUDIs were operated side-by-side, one with 37 mm diameter baked aluminum foils and a quartz backup filter for elemental and organic carbon measurements, and one with pre-washed, 37 mm diameter PFA Teflon sheets for mass, sulfate, and nitrate measurements. Each MOUDI sampled at 30 l/min through a California Air and Industrial Hygiene Laboratory (AIHL) cyclone which has a 2.2 μm cutpoint at this flow rate[11].

These units were operated from 0900 to 1600 MST to correspond to the daytime fine particle measurements. Flow rates were controlled by the impactor stages themselves, which act as critical orifices. Flow rates were verified by relating volumetric flow measured with a dry test meter to the pressure drop across several of the lower MOUDI stages. This pressure drop was measured after each sample changeout to verify that leaks are not present in the impactor stack. Samples were changed before and after the daytime sampling period every two days, following the same schedule as the sequential filter sample changeout. An electronic timer was set to start and stop sampling at the prescribed periods. Impactor jets were cleaned in an ultrasonic bath every other changeout to prevent clogging by large particles. Filter substrates were loaded and unloaded onto the impaction plates in the field laboratory to minimize contamination. Samples were kept at less than 4 °C from the time of unloading until they were presented to chemical analysis.

PARTICLE AND GAS EXTINCTION EFFICIENCIES

The total extinction is divided into five components: 1) light absorption by gases; 2) light absorption by particles; 3) light scattering by gases; 4) light scattering by coarse particles; and 5) light scattering by fine particles. Scattering efficiencies are needed for each of these components to translate concentrations of atmospheric constituents into light extinction.

Light Absorption by Gases

Nitrogen dioxide (NO_2) is the only gas likely to be present in Denver which causes significant absorption of visible light. The absorption coefficient of nitrogen dioxide has been determined[12], and has the value of 0.17 Mm^{-1} per $\mu g/m^3$ at a wavelength of 550 nm, which is the wavelength for the transmissometer measurements. The light absorption by gases is determined in this study by measuring the NO_2 concentration and then multiplying this concentration by the absorption coefficient.

Light Absorption by Particles

Light absorption by particles in urban areas is predominantly caused by elemental carbon. Unweighted least squares estimates of the absorption efficiency derived from simultaneous measurements of Teflon filter absorption and elemental carbon concentrations gave an absorption efficiency of 9.1±0.09 m^2/g ($r = 0.94$) for elemental carbon. This value for the elemental carbon absorption efficiency is in good agreement with the value of 9.0 m^2/g used in the RESOLVE study[13].

Light Scattering by Gases

The magnitude and wavelength dependence of light scattering by gases (Rayleigh scattering) are well known as a function of the air density[14,15]. The magnitude of scattering by pure air varies with the barometric pressure and temperature. On the average, it has a value of 9.9 Mm^{-1} at a wavelength of 550 nm in Denver and varies by about ±5%. The transmissometer measures total extinction at a wavelength of 550 nm, but the integrating nephelometer measures light scattering by particles for a range of wavelengths near 530 nm. At this shorter wavelength, the average value of light scattering by gases is 10.7 Mm^{-1}. This slight discrepancy is well within measurement uncertainty, and the 9.9 Mm^{-1} value is used to represent Rayleigh scattering.

Light Scattering by Coarse Particles

Light scattering by coarse particles is the least accurately known component of extinction. The only data for coarse particle concentrations which can be compared with the fine particle measurements of this Study were from PM_{10} measurements by the Colorado Department of Health at another site in the network. Samples were taken every third day using a high-volume sampler with a SA-321A PM_{10} inlet. Multiple linear regressions were performed to see if the PM_{10} data could be predicted from the collocated fine particle mass and chemistry data.

It was found that on the average, the PM_{10} mass was (2.6±1.0) times as large as the fine particle mass. The following equation was derived from unweighted linear regression of the coarse particle mass concentration (PM_{10} minus $PM_{2.5}$) on the $PM_{2.5}$ (fine) mass and iron concentrations.

$$\text{coarse mass} = (3.07\pm6.7) + (0.308\pm0.22) \times PM_{2.5} + (187\pm50) \times (\text{iron}) \quad (r = 0.64)$$

All units in this equation are $\mu g/m^3$. The mass of fine particles ($PM_{2.5}$) is a surrogate for meteorological stagnation as well as a direct indicator of the contribution of fine particles to PM_{10}, and iron is used as a predictor of the contribution of crustal materials to the coarse particle fraction.

Trijonis et al.[13] summarized efficiencies from a variety of references and used a value of 0.6 m^2/g. White and Macias[16] performed regression analyses of data obtained at Spirit Mountain located at the southern tip of Nevada and obtained a value near 0.2 m^2/g for the extinction efficiency of crustal materials. The extinction efficiency of coarse particles is not well known and can be quite variable. The 0.6 m^2/g adopted by Trijonis et al.[13] is based on a review of several previous measurements and is used here. The contribution to extinction derived from a highly uncertain coarse particle scattering efficiency and an equally uncertain estimate of coarse particle mass concentrations must also be highly uncertain. Contributions from coarse particle scattering are not expected to be any better than a factor of two, and they will only give an indication of whether or not this component of light extinction is important enough to submit to further study in Denver.

Light Scattering by Fine Particles

White[17] and Sloane[18] demonstrate that fine particle scattering efficiencies for different chemical species are not constant, but depend on other species in a fine particle. This is the case because the light scattering properties of a particle are strongly affected by its size. Adding or removing a portion of one species may change the size of the particle, and this will change the light scattering efficiencies of all of the remaining species.

Two methods were used to estimate how the $PM_{2.5}$ light scattering by an aerosol sample changes if the concentration of one of the species is changed: 1) regression analysis[19]; and 2) deterministic calculations based on the chemical analysis of MOUDI samples[20]. The details of the process applied to these data are lengthy and are reported in Watson et al.[3]. The regression analysis was performed using a least squares multiple regression algorithm corrected for measurement error[21] on nephelometer scattering and selected SFS chemical concentrations. The deterministic calculations used the model developed by Sloane [19,21,22] applied to ambient relative humidity and chemically-speciated particle size distributions obtained from the MOUDI. Combining these two approaches resulted in a chemical-specific $PM_{2.5}$ scattering efficiency, b_{scat}, of:

$$b_{scat} = [(0.53+0.11RH)\pm30\%]C_{SO4} + [(0.32+0.066RH)\pm30\%]C_{OC}$$

$$+[(0.41+0.085RH)\pm30\%]C_{NO3} + [1.0\pm30\%]C_{RES}$$

where C_{RES} - $C_{PM25} - 1.375C_{SO4} - 1.29C_{NO3} - C_{OC}$
C_{PM25} - $PM_{2.5}$ mass concentration in $\mu g/m^3$
C_{SO4} - $PM_{2.5}$ sulfate concentration in $\mu g/m^3$
C_{NO3} - $PM_{2.5}$ nitrate concentration in $\mu g/m^3$
C_{OC} - $PM_{2.5}$ organic carbon concentration in $\mu g/m^3$
RH - Relative humidity in percent

These chemical-specific fine particle scattering efficiencies are similar in magnitude to those used by Trijonis et al.[13].

RESULTS

Seven and seventeen hour averages were calculated from the hourly values obtained from the transmissometer, the nephelometer, and the nitrogen dioxide monitor. These averages are needed for comparison with the daytime (seven hour average) and nighttime (seventeen hour average) chemical measurements.At least four valid hourly values were required for the seven hour averages and at least nine valid hourly values were required for the seventeen-hour averages. The precision of each average was set equal to the standard error of the average.

PATH measurements of light extinction were derived from transmissometer averages. POINT measurements of light extinction were calculated by summing the nephelometer scattering, Teflon filter absorption, the product of nitrogen dioxide concentration and absorption efficiency, and Rayleigh scattering. CHEMICAL measurements of light extinction were calculated by summing the Rayleigh scattering, the nitrogen dioxide absorption, elemental carbon absorption, coarse particle scattering, and chemical-specific fine particle scattering components derived from the relationships specified in the prior sub-section. The measurement precisions for all variables were propagated by addition in quadrature for these sums.

Figure 1 shows scatterplot comparisons of the valid PATH, POINT, and CHEMICAL measures of visibility extinction for all of the seven and seventeen hour averages available in the data set. A more quantitative examination of the paired data is presented in Table I. The equivalence, bias, and predictability of paired measurements can be defined by a number of different performance measures. The notes to Table I define the performance measures and their expected values. Several of these measures are calculated in Table I for different subsets of the light extinction data.

DISCUSSION

A cursory examination of Figure 1 gives the impression that, despite some scatter, the three measures of light extinction are fairly equivalent. The scatter of data pairs in the POINT/CHEMICAL plot is less than that in the POINT/PATH and CHEMICAL/PATH plots. This is to be expected, since the estimates of absorption have two components in their sum (nitrogen dioxide absorption and

Rayleigh scattering) and because the instruments were located right next to each other. There are probably inhomogeneities in the extinction along the transmissometer sight path which do not register on the point measurements.

Table I shows comparison performance measures for all data and a subset of data which were acquired after the nephelometers were operated at ambient temperature. The measures have been calculated for each subset with and without data pairs which exceeded three times the sum of their estimated precisions. The distribution in Table I shows that approximately 10% of the PATH/POINT data pairs were outliers, but only 2 to 3% of the CHEMICAL/POINT and CHEMICAL PATH pairs were outliers. The collocated precision of the measurements is approximately 30 Mm^{-1}, and this is approximately twice the RMSE derived from the individual measurement precision estimates. The performance measures improve substantially when the outliers are removed. These outlier pairs have been identified and are currently under study to determine the reasons for the large differences.

With outliers removed, there is little difference between the performance measures for all data and those taken after 11/20/87. Relative humidities were relatively low during the first two weeks of monitoring, and the large temperature differences between the nephelometer sample chamber and the ambient air do not appear to be significant. When outliers are ignored, each slope is within three standard errors of unity. The POINT/PATH and CHEMICAL/PATH slopes are within 2% of each other. The CHEMICAL/POINT slope is a little lower, but not significantly so.

The intercepts are significant and show a slight negative bias of the POINT with respect to the PATH measurement and a slight positive bias of the CHEMICAL versus path measurement. These biases also show up in the average differences, but the bias is much less than either the collocated or the RMSE precisions. The % distributions show that the CHEMICAL/PATH comparisons have the largest percentage of pairs for which differences fall with one or two standard deviations. Even with outliers included, 70% of the CHEMICAL/PATH pairs fall within one overlapping precision interval. Only about 50% of the POINT/PATH and CHEMICAL/POINT measurement pairs differ by less than one overlapping precision interval.

CONCLUSIONS

The conclusions to be drawn from this comparison are:

- Time-averaged light extinction derived from chemical measurements and reasonable estimates of extinction efficiency are comparable to collocated point measurements of visibility extinction.

- Both point visibility and point chemical measurements of light extinction are comparable to extinction measured with a transmissometer over a 3 km elevated sight path in an urban environment.

REFERENCES

1. Watson, J.G., J.C. Chow, L.W. Richards, S.R. Anderson, J.E. Houck, and D.L. Dietrich (1988a). "The 1987-88 Metro Denver Brown Cloud Air Pollution Study Volume I: Program Plan." DRI Document No. 8810.1F1, prepared for the Greater Denver Chamber of Commerce, Denver, CO, by Desert Research Institute, Reno, NV.

2. Watson, J.G., J.C. Chow, L.W. Richards, S.R. Anderson, J.E. Houck, and D.L. Dietrich (1988b). "The 1987-88 Metro Denver Brown Cloud Air Pollution Study Volume II: Measurements." DRI Document No. 8810.1F2, prepared for the Greater Denver Chamber of Commerce, Denver, CO, by Desert Research Institute, Reno, NV.

3. Watson, J.G., J.C. Chow, L.W. Richards, S.R. Anderson, J.E. Houck, and D.L. Dietrich (1988b). "The 1987-88 Metro Denver Brown Cloud Air Pollution Study Volume III: Data Interpretation." DRI Document No. 8810.1F3, prepared for the Greater Denver Chamber of Commerce, Denver, CO, by Desert Research Institute, Reno, NV.

4. Ruby, M.G., and A.P. Waggoner (1981). "Intercomparison of Integrating Nephelometer Measurements." *Environ. Sci. Technol.*, 15, 109.

5. Ensor, D.S., and A.P. Waggoner (1970). "Angular Truncation Error in the Integrating Nephelometer." *Atmos. Environ.*, 4, 481.

6. Rabinoff, R.A., and B.M. Herman (1973). "Effect of Aerosol Size Distribution on the Accuracy of the Integrating Nephelometer." *J. Appl. Meteorol.*, 12, 184.

7. Mudgett, P.S., and L.W. Richards (1971). "Multiple Scattering Calculations for Technology, I." *Appl. Op.*, 10, 1485.

8. Mudgett, P.S., and L.W. Richards (1972). "Multiple Scattering Calculations for Technology, II." *J. Colloid Interface Sci.*, 39, 551.

9. Winer, A.M., J.W. Peters, J.P. Smith, and J.N. Smith (1974). "Response of Commercial Chemilumiescent NO-NO_x Analyzers to Other Nitrogen Containing Compounds." *Environ. Sci. Technol.*, 8, 1118.

10. U.S. Environmental Protection Agency (1977). "Quality Assurance Handbook for Air Pollution Measurements Systems, Volume II: Ambient Air Specific Methods." EPA-600/4-77-027a, U.S. Environmental Protection Agency, Research Triangle Park, NC.

U.S. EPA (1977c). "Users Guide for Single Source (CRSTER) Model. EPA-450/2-79-013, U.S. Environmental Protection Agency, Research Triangle Park, NC.

11. John, W., and G. Reischl (1978). "A Cyclone for Size-Selective Sampling of Ambient Air." AIHL Report No. 187, California Air Industrial Hygiene Laboratory, Berkeley, CA.

12. Dixon, J.K. (1940). "The Absorption Coefficient of Nitrogen Dioxide in the Visible Spectrum." *J. Chem. Phys.*, 8, 157.

13. Trijonis, J., M. McGown, M. Pitchford, D. Blumenthal, P. Roberts, W. White, E. Macias, R. Weiss, A. Waggoner, J. Watson, J. Chow and R. Flocchini (1988). "The RESOLVE Project Final Report: Visibility Conditions and Causes of Visibility Degradation in the Mojave Desert of California." Report NWC TP 6869, prepared for the Naval Weapons Center, China Lake, CA, by Santa Fe Research Corporation, Bloomington, MN.

14. Penndorf, R. (1957). "Tables of the Refractive Index for Standard Air and the Rayleigh Scattering Coeffficient for the Spectral Region Between 0.2 and 20 μm and Their Applications to Atmosphere Optics." *J. Opt. Soc. Am.*, 47, 176.

15. Edlen, B. (1953). "The Dispersion of Standard Air." *J. Opt. Soc. Am.*, 43, 339.

16. White W.H., and E.S. Macias (1988). "Light Scattering by Haze and Dust at Spirit Mountain, Nevada." Presented at 81st APCA Annual Meeting, Dallas, Texas. Air Pollut. Control Assoc., Pittsburgh, PA.

17. White, W.H. (1986). "On the Theoretical and Empirical Basis for Apportioning Extinction by Aerosols: A Critical Review." *Atmos. Environ.*, 20, 1659.

18. White, W.H., and P.T. Roberts (1977). "On the Nature and Origins of Visibility-Reducing Aerosols in the Los Angeles Air Basin." *Atmos. Environ.*, 11, 803.

19. Sloane, C.S. (1986). "Effect of Composition on Aerosol Light Scattering Efficiencies." *Atmos. Environ.*, 20, 1025.

20. White W.H. (1989). "Heteroscedasticity and the Standard Errors of Regression Estimates." in *Transactions: Receptor Models in Air Resources Management* edited by J.G. Watson, Air and Waste Management Association, Pittsburgh, PA, p. 226.

21. Sloane, C.S. (1984). "Optical Properties of Aerosols of Mixed Composition." *Atmos. Environ.*, 18, 871.

22. Sloane, C.S. (1985). "Change in Aerosol Optical Properties with Change in Chemical Composition." Presented at 78th Annual Meeting, Detroit, MI. Air Pollut. Control Assoc., Pittsburgh, PA.

23. Watson, J.G., J.A. Cooper and J.J. Huntzicker (1984). "The Effective Variance Weighting for Least Squares Calculations Applied to the Mass Balance Receptor Model." *Atmos. Environ.*, 18, 1347.

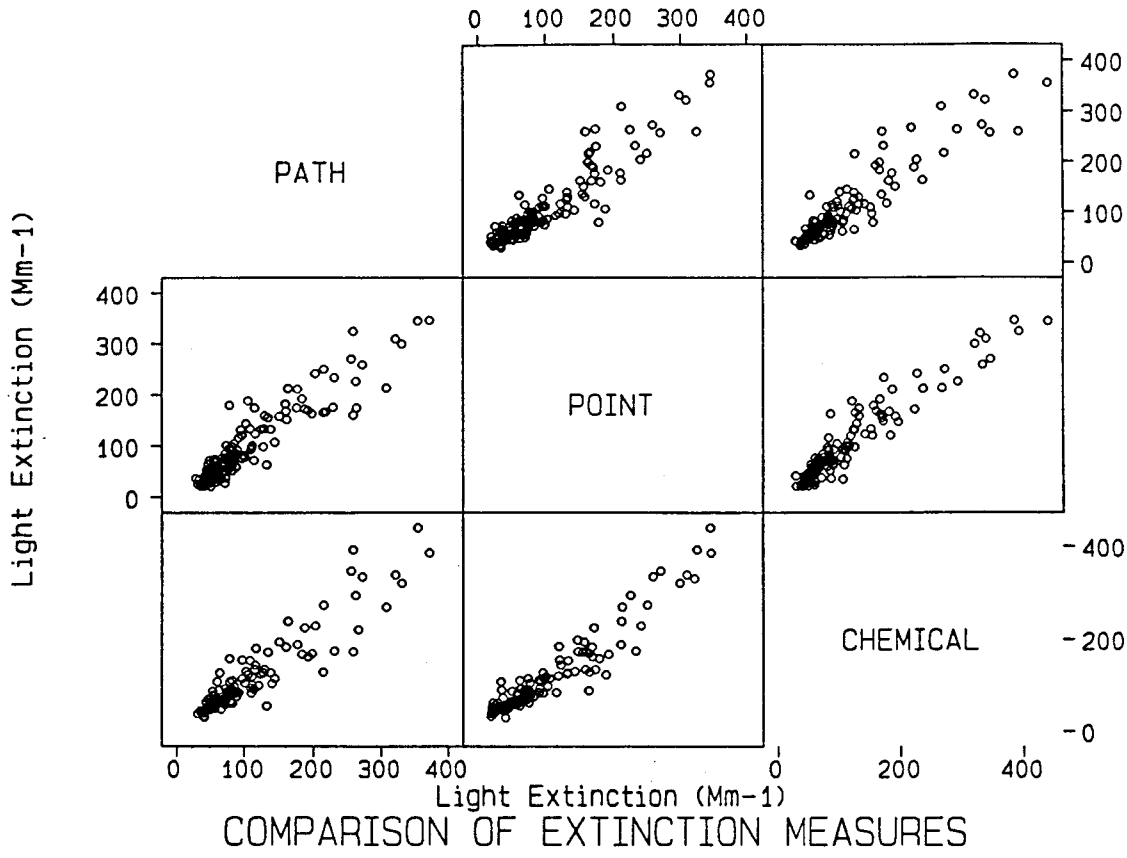

Figure 1. Scatterplot comparison of light extinction measured by three different methods.

PATH-Seven and seventeen (day and night) averages of hourly transmissometer measurements along a 2.7 km sight path.

POINT-Sum of seven and seventeen hour averages of: 1) nephelometer particle scattering; 2) Rayleigh scattering; 3) Teflon filter absorption; and 4) nitrogen dioxide absorption.

CHEMICAL-Sum of seven and seventeen hour averages of: 1) elemental carbon absorption; 2) nitrogen dioxide absorption; 3) fine particle sulfate scattering; 4) fine particle nitrate scattering; 5) fine particle organic carbon scattering; 6) fine particle remaining mass scattering; 7) coarse particle scattering; and 8) Rayleigh scattering.

Table I
Comparison Performance Measures for PATH, POINT, and CHEMICAL Light Extinction Values

Data[a] Compared	Dependent[b] Variable(Y)	Independent[b] Variable(X)	Slope[c]	Intercept[c] (Mm^{-1})	Correlation Coeff. (r)[c]	No. of Pairs	Average Ratio (Y/X)[d]	% Distribution[e] <1σ	1-2σ	2-3σ	>3σ	Average Difference[f] (Mm^{-1})	Collocated Precision[f] (Mm^{-1})	Y RMSE[g] (Mm^{-1})	X RMSE[g] (Mm^{-1})
All Data	POINT	PATH	1.01+- 0.02	-8.69+-1.50	0.872	135	0.92+-0.28	46,	33,	12,	10	-7.02	28.16	10.57	17.17
	CHEMICAL	PATH	0.91+- 0.03	9.07+-2.32	0.895	118	1.07+-0.25	69,	24,	5,	2	5.99	31.50	13.83	17.15
	CHEMICAL	POINT	0.89+- 0.02	17.36+-1.84	0.917	119	1.26+-0.41	54,	33,	11,	3	13.12	26.44	13.95	11.10
All Data	POINT	PATH	0.99+- 0.02	-3.11+-1.67	0.908	122	0.95+-0.25	51,	36,	13,	0	-5.13	26.36	10.99	17.98
without	CHEMICAL	PATH	0.96+- 0.03	5.77+-2.44	0.911	116	1.07+-0.24	71,	24,	5,	0	6.18	29.85	13.86	17.24
Outliers	CHEMICAL	POINT	0.93+- 0.02	14.98+-1.88	0.936	116	1.25+-0.37	55,	34,	11,	0	14.05	23.71	13.96	11.17
All Data	POINT	PATH	0.98+- 0.02	-8.36+-1.56	0.862	115	0.88+-0.26	41,	36,	12,	11	-9.64	27.51	10.53	17.53
After	CHEMICAL	PATH	0.89+- 0.03	8.87+-2.41	0.910	98	1.05+-0.22	69,	24,	5,	1	4.54	32.07	13.99	17.64
11/20/87	CHEMICAL	POINT	0.88+- 0.02	18.65+-1.91	0.916	102	1.30+-0.43	49,	35,	13,	3	14.94	27.39	14.10	11.04
All Data	POINT	PATH	0.97+- 0.03	-2.58+-1.75	0.901	102	0.92+-0.22	46,	40,	14,	0	-7.71	25.42	11.02	18.52
After	CHEMICAL	PATH	0.95+- 0.03	5.87+-2.54	0.917	97	1.06+-0.22	70,	25,	5,	0	5.48	30.86	14.00	17.70
11/20/87 without Outliers	CHEMICAL	POINT	0.93+- 0.03	16.10+-1.96	0.937	99	1.29+-0.38	51,	36,	13,	0	16.09	24.22	14.12	11.12

[a] Nephelometers were operated at ambient temperatures after 11/20/87. Internal nephelometer temperatures were approximately 10 °C higher than ambient temperatures prior to this date. Outliers pairs are those for which the difference between values is greater than three times the sum of precisions.

[b] Variables used as the dependent (Y) and independent variable (X) in performance measures.

[c] Linear regression parameters were calculated using effective variance weighted least squares[23] which incorporates the precisions of both variables into the weighting of each value. The effective variance also propagates these precisions to provide the standard errors which are reported with parameter. Slope of one (within three standard errors), intercept of zero (within three standard errors), and correlations which exceed 0.9 are considered good comparisons.

[d] Average and standard deviation of the ratios of the dependent over independent variables.

[e] The percent fraction of measurements which fall into different numbers of overlapping precision intervals. In the ideal situation, more than 66% of the values should fall within the sum of the 1σ intervals for the paired measurements. Less than 30% should fall within the sum of the 1 to 2σ intervals, less than 5% should fall within the sum of the 2 to 3σ intervals, and less than 1% should exceed the sum of the 3σ intervals. When fractions in the 2-3σ and >3σ categories exceed 5% and 1%, some of the values may be outliers, or the sampling systems are not equivalent. The effects of outliers have been determined by recalculating the comparison measures with pairs for which the difference exceeds 3σ removed.

[f] Average and standard deviation of the difference between the paired measurement. The collocated precision is the standard deviation of the difference. When the average difference exceeds its standard deviation reported in column 10, there is a bias between the samplers. The sign of the average difference shows the direction of the bias.

[g] Root mean square error--square root of the average of the squares of the measurement precisions. These precisions can be compared to the collocated precision.